

# The Synergistic Effect of Aluminum Hypophosphide and Nanosilica on Flame-Retarded Ethylene–Propylene–Diene Monomer Rubber

Zongtao Wang, Xian Zhang, Chao Bao, Qunyue Wang, Yong Qin, Xingyou Tian

Key Laboratory of Materials Physics, Institute of Solid State Physics, Chinese Academy of Sciences, Hefei 230031, People's Republic of China

Received 18 May 2011; accepted 11 August 2011

DOI 10.1002/app.35460

Published online 21 November 2011 in Wiley Online Library (wileyonlinelibrary.com).

**ABSTRACT:** The influence of aluminum hypophosphide (AlHPi) and nanosilica on the flame-retardant and mechanical property of ethylene–propylene–diene monomer (EPDM) rubber was evaluated by limiting oxygen index, and the value of tensile strength and elongation at break. The results show that the introduction of nanosilica into the EPDM/AlHPi blends can not only further improve the flame-retardant property but also improve the tensile strength and elongation at break significantly, showing a synergistic effect between AlHPi and nanosilica. The flame-retardant mechanism was further studied by X-ray diffraction (XRD), thermogravimetric (TG) analysis, differential scanning calorimetry (DSC), and scanning electron microscope (SEM). The results of XRD and TG–DSC indicate that AlHPi will melt along with oxidation at about 337°C, which is helpful to full contact with nanosilica and to enhance the

interaction between them; and will further recrystallize above 540°C, which is benefited to enhance the mechanical strength of char layer. The char morphological study by SEM shows that the char layer for the sample with both AlHPi and nanosilica is strong, more uniform and dense, and the scale of the holes in the char layer is smaller compared with the char layer of samples with AlHPi or nanosilica alone. The TG–DSC results show that the sample with both AlHPi and nanosilica has the weakest weight loss rate and heat release rate, compared with the samples with either of them, which is another evidence of the synergistic flame retardant effect between AlHPi and nanosilica. © 2011 Wiley Periodicals, Inc. *J Appl Polym Sci* 124: 3487–3493, 2012

**Key words:** flame retardance; rubber; aluminum hypophosphide; silicas; synergistic effect

## INTRODUCTION

Ethylene–propylene–diene monomer (EPDM) rubber is widely used in many areas such as automobile manufacture, architecture, cable industry, etc, because of its unique properties such as high temperature resistance, weather resistance, ozone resistance, and excellent insulating properties.<sup>1–3</sup> However, EPDM is extremely flammable, which restricts its application in many fields and leaves security risk without adequate flame-retardant treatment. Therefore, the development of the flame-retardant EPDM composite has been the focus of research in recent years.<sup>1,4</sup>

As halogen-containing flame retardants produce large amounts of smoke and toxic gases during combustion,<sup>5</sup> nowadays, the research is focused on halogen-free flame retardants. Metal hydroxides,<sup>4,6,7</sup> for example, magnesium hydroxide and aluminum hydroxide, are commonly used in EPDM composite. However, a high loading (>50 wt %) was required to obtain an adequate level of flame-retardant property,

which lead to the decrease of the mechanical property. Recently, phosphorus-containing flame retardants have caused a lot of research interest. For example intumescent flame retardants (IFR)<sup>1,2</sup> usually comprise phosphorus-containing additives such as ammonium polyphosphate and melamine phosphate. Unfortunately, the conventional IFR additives also have disadvantages such as bad matrix compatibility, poor mechanical properties, moisture sensitivity, and migration.<sup>8,9</sup> The recently developed and commercialized metal phosphinates (MPi) belong to a novel class of phosphorous-containing flame retardants,<sup>10</sup> with some excellent properties such as thermal stability and low water solubility, which is a requirement for practical application.<sup>11,12</sup> They show effective flame-retardant function when used in polyesters and polyamide, especially glass-fiber reinforced polyesters<sup>5,11,13</sup> and polyamide,<sup>10</sup> but to the author's knowledge, there is little information available in the published reports about the application of MPi in EPDM formulations. This is probably due to the low flame-retardant efficiency and the negative influence on the mechanical property of the matrix when they are used alone.

Nanosilica is commonly used as an additive in the polymer to enhance the mechanical property of the

Correspondence to: X. Tian (xytian@issp.ac.cn).

**TABLE I**  
**Formulations of EPDM/AlHPi/SiO<sub>2</sub> Composites**

Code	EPDM/phr	SiO <sub>2</sub> /phr	AlHPi/phr	DCP/phr
EPDM0-0	100	0	0	3
EPDM0-15	100	0	15	3
EPDM0-30	100	0	30	3
EPDM20-0	100	20	0	3
EPDM20-15	100	20	15	3
EPDM20-30	100	20	30	3

matrix. Previous researches also show that nanosilica has some extent of flame-retardant effect when added in polymer.<sup>14,15</sup> As mentioned above, MPi is surprisingly effective on the flame retardancy of polyesters and polyamide with the presence of glass fiber, so a synergistic effect between MPi and nanosilica can be expected, as both nanosilica and glass fiber belong to a kind of inert additive with similar chemical composition.

In this study, a kind of EPDM/AlHPi/nanosilica ternary composite was prepared, and the effect of AlHPi and nanosilica on the flame retardant and mechanical property of EPDM was evaluated. To further study the flame-retardant mechanism, as uncertainties about the flame-retardant mechanism of MPi still exist,<sup>10,11,13</sup> the authors investigated the thermal degradation process and char morphology of the samples by X-ray diffraction (XRD), thermogravimetric (TG), differential scanning calorimetry (DSC), and scanning electron microscope (SEM).

## EXPERIMENTAL

### Materials

Ethylene-propylene-diene monomer rubber (EPDM Vistalon<sup>TM</sup> 7001) containing 73 wt % of ethylene and 5 wt % of ethylidene norbornene was supplied by ExxonMobil. Aluminum hypophosphite (AlHPi) was bought from Shaoxing Haicheng Chemical, China, and was used as received. Nanosilica was supplied by Shanghai Chlor-alkali, China. The average particle size and specific surface area were 13 nm and 200 m<sup>2</sup>/g, respectively. It was used without further treatment. Dicumyl peroxide (DCP), powder 40% on whiting carrier, was bought from AKZO NOBEL Cross-linking Peroxides (Ningbo, China).

### Sample preparation

The pure EPDM was processed on the open mill instrument at 90°C for 5 min, and then the additives were added in the order of AlHPi, nanosilica, and DCP. Then they were cured on the platen press under 11 MPa pressure at 160°C for the time of  $t_{c90}$ , obtained from the Moving Die Rheometer (GOTECH, China). The resulting sample formulations were listed in Table I.

## Analysis of samples

### Flammability test

The limiting oxygen index (LOI) value was measured using a JF-3 LOI test instrument (Jiangning Analytical Instrument, China), according to ASTM D 2863 with sample dimensions of 100 mm × 6.5 mm × 3 mm. All measurements were made thrice for each sample.

### Mechanical measurement

The mechanical property study was performed on an instron universal tester (CMT 4204, SANS, China) according to the GB/T 528-1998 standard, with a cross-head speed of 500 mm/min. All measurements were made thrice for each sample.

### TG-DSC test

The TG-DSC measurement was performed on a SDTQ600 TG-DSC analyzer at a heating rate of 10°C/min, heating from 50 to 700°C in air with a flow rate of 40 mL/min. Meanwhile, the corresponding heat flow during the TG-test was measured by the DSC accessory. For the sample of AlHPi, the TG-DSC curve in nitrogen was also measured at the same heating rate and temperature region.

### XRD test

The XRD patterns were obtained from the X' Pert Pro MPD diffractometer (Philips, Holland) with the Cu K $\alpha$  radiation ( $\lambda = 1.5408 \text{ \AA}$ ), the scattering intensities were recorded from 2 $\theta$  scans in the range of 10–60°. The measurements were performed when the samples were cooled to room temperature.

### SEM analysis

The char layers were collected after burning in the LOI instrument<sup>16,17</sup> and were characterized by a Sirion 200 type SEM.

## RESULTS AND DISCUSSION

### Flame-retardant property

The LOI values of different samples are shown in Figure 1. It can be seen that the LOI value of EPDM keeps increasing with the content of AlHPi, and reaches 22.1% when 30 phr of AlHPi is added. When 20 phr of nanosilica is introduced into the EPDM/AlHPi system, the LOI value is further improved, for example, the LOI value reaches 25.3% for the sample of EPDM20-30, although adding nanosilica into the pure EPDM only results in a slight increase of the LOI value. Meanwhile, the difference of LOI value between the samples with and

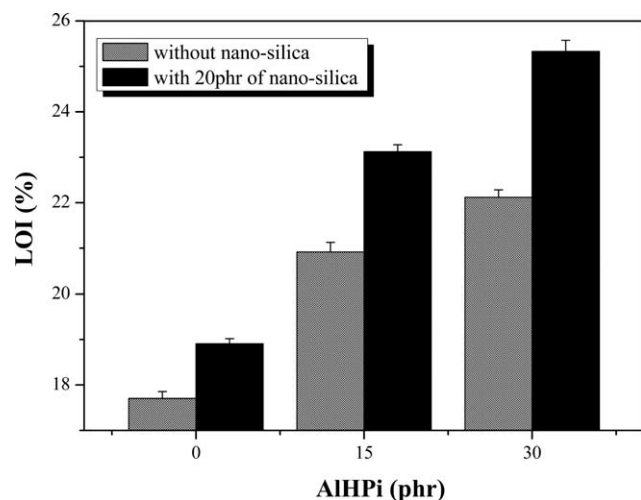


**Figure 1** The LOI values versus the AIHPi loading for EPDM/AIHPi/nanosilica composites.

without nanosilica is more obvious with a higher loading of AIHPi. The results indicate that there is a synergistic flame-retardant effect between AIHPi and nanosilica, and the synergistic effect is more obvious with a higher content of AIHPi.

### Mechanical property

Considering practical industry requirement, it is necessary to investigate the effect of the flame retardants on the mechanical property of EPDM. It can be seen from Figure 2(a,b) that the introduction of AIHPi alone into the EPDM composites results in slight decrease both in the tensile strength and elongation at break. However, the mechanical properties increase significantly for the samples EPDM20-15 and EPDM20-30 by the addition of nanosilica, especially, the values of tensile strength are 3.6–4.2 times that of the samples EPDM0-15 and EPDM0-30. Similar results have been reported by other researchers,<sup>18–20</sup> and the reason could be attributed to the enhanced interaction between nanosilica and the matrix due to large specific surface area of nanosilica.<sup>19,21–23</sup> This is very important for the practical usage of EPDM as cable materials and so on.

### Mechanism study

#### Analysis of AIHPi

To better understand the synergistic flame-retardant mechanism of nanosilica and AIHPi in EPDM composite, the authors investigated the thermal oxidation behavior of the AIHPi by XRD and TG–DSC, as shown in Figures 3 and 4(a–d). The results show that the decomposition process of AIHPi can be divided into three stages in the entire temperature region: I, from 20 to 320°C; II, from 320 to 540°C; III,

above 540°C. In the first stage, the XRD results indicate that the characteristic diffraction peaks of AIHPi become weak with the increase of temperature. At the same time, the TG–DSC curves in both air and nitrogen show that about 6 wt % of AIHPi is lost between 230 and 317°C and there is no apparent heat release in the DSC curve. It can be inferred from the results that only the decomposition of AIHPi occurs in this stage. In the second stage, the TG–DSC curve in air shows a sharp weight increase peak at around 320°C, followed by a slow-weight decrease until 540°C. Meanwhile, there is a sharp heat release peak at around 320°C in the DSC curve,

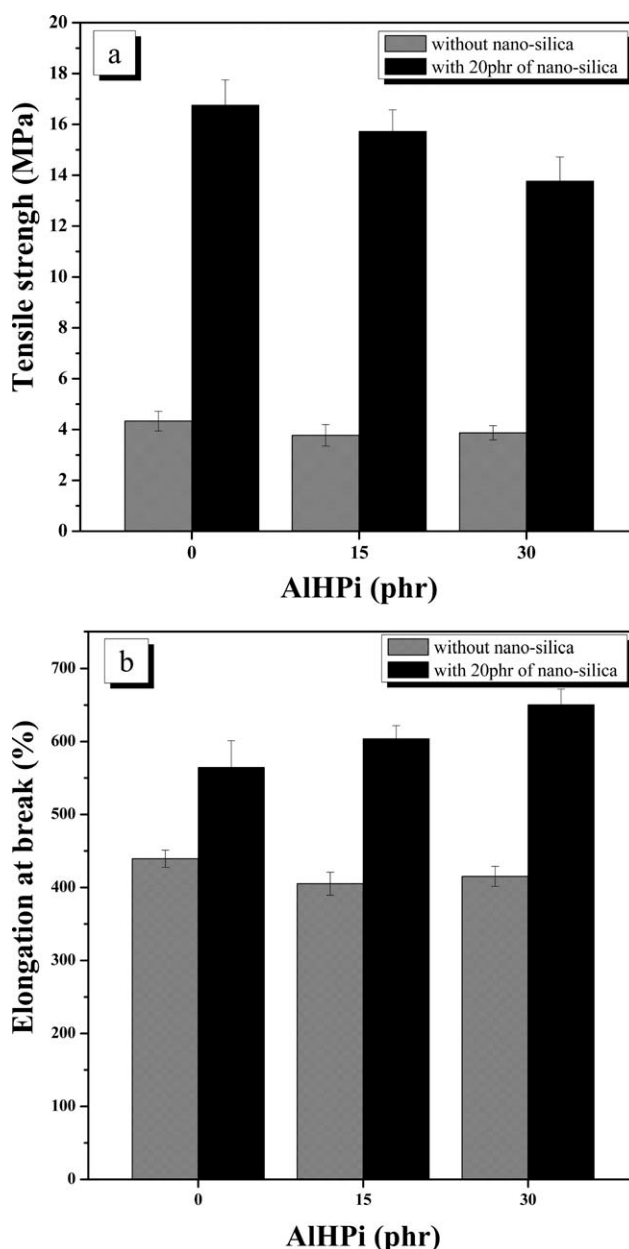


**Figure 2** Mechanical properties versus the AIHPi loading for EPDM/AIHPi/nanosilica composites: (a) tensile strength. (b) Elongation at break.

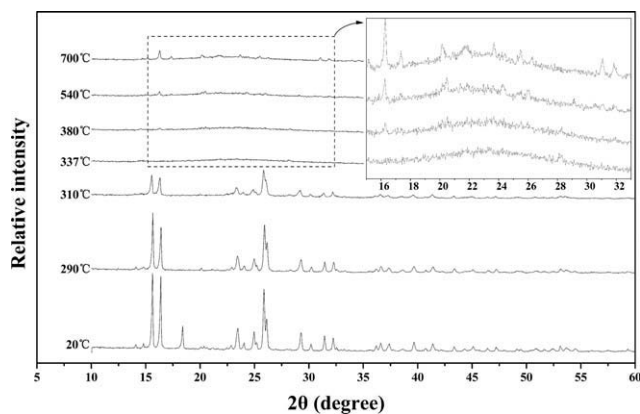


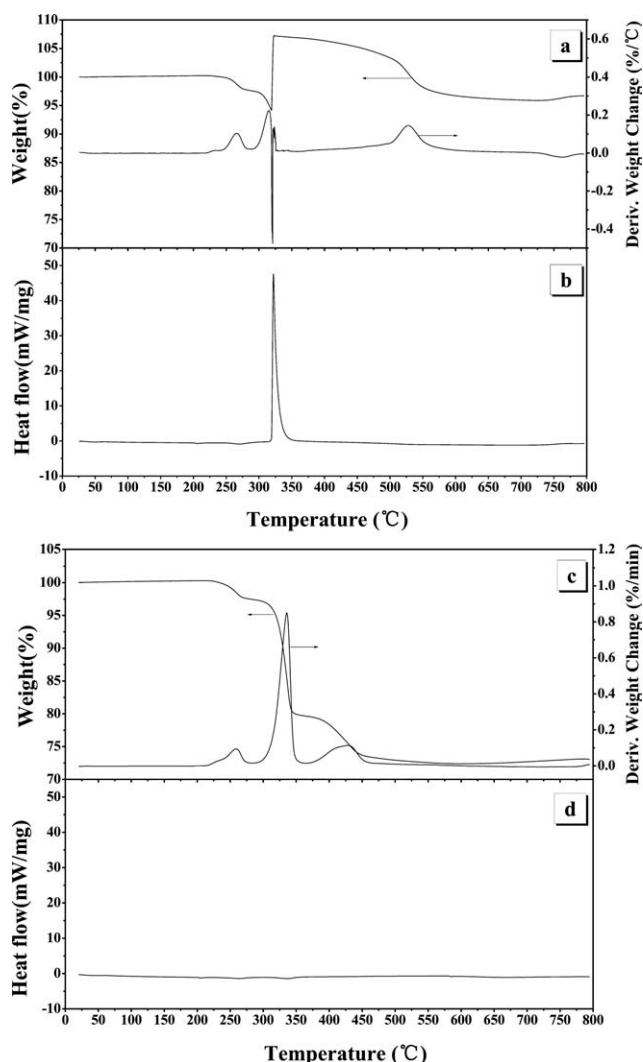
**Figure 3** XRD results of AIHPi at different temperatures in air.

which is attributed to the oxidation of AIHPi. At the same time, the diffraction peaks in the XRD curve disappear at 337°C, which is probably due to the melt of AIHPi along with the oxidation. In contrast, there is neither weight increase nor heat release for the TG–DSC curve in nitrogen, which further proved the weight increase in air atmosphere resulted from the oxidation of AIHPi. It is important for the flame retardant to melt before charring because it allows the flame retardant to flow and form a more uniform char layer, especially, it is helpful to full contact with nanosilica, and to enhance the interaction between them.<sup>24–29</sup> In the third stage, interestingly, new peaks appear above 540°C as shown in the XRD curve. The weight value in the TG-curve in air almost remains constant and there is no heat release in this stage. These results may indicate that AIHPi has undergone a process of recrystallization in this stage. This is benefited to enhance the mechanical strength of the char and to withstand the attack of the rising bubbles during combustion. In addition, it had to be noted that 96 wt % of residue was left at 800°C and there is no apparent mass release during the TG–DSC test in air. On the basis of the above result, it can be inferred that AIHPi mainly act in a condensed-phase flame-retardant mechanism.

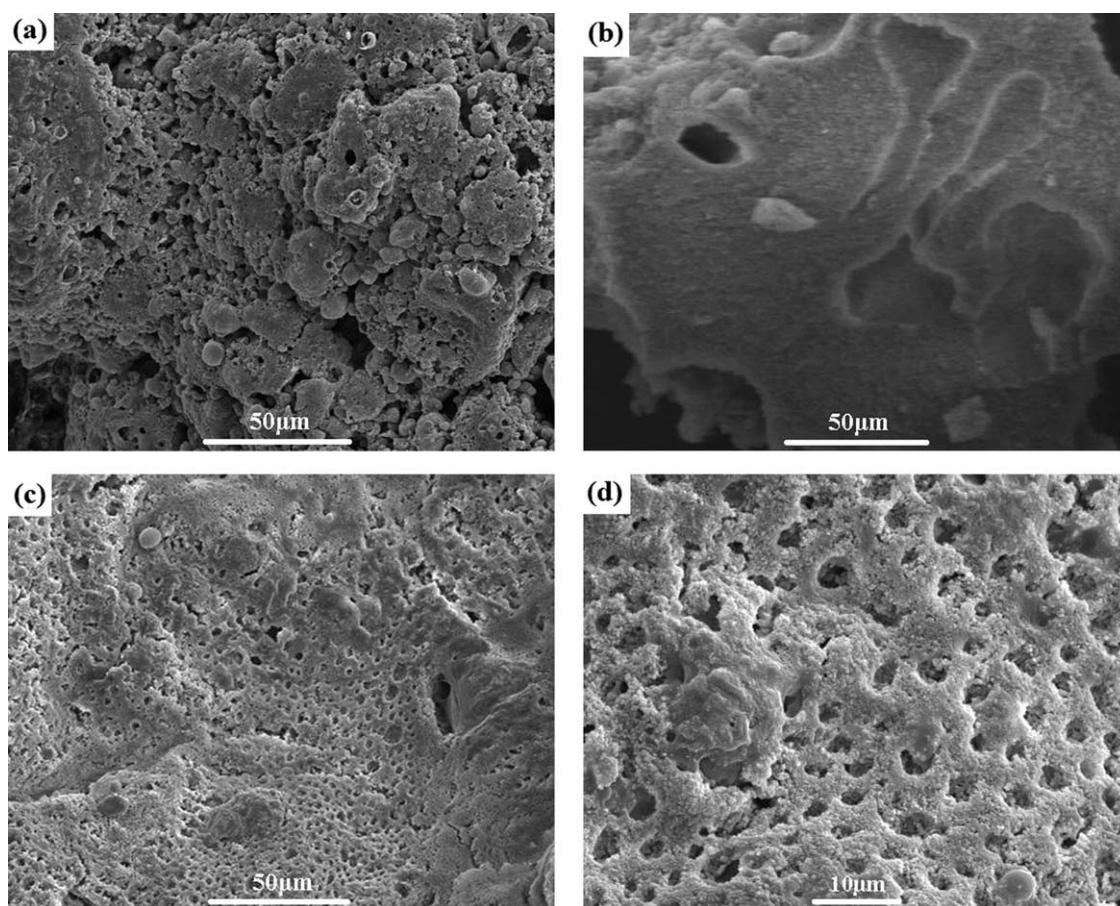
#### Char morphology analysis

Figure 5(a–d) shows the char morphology of different samples. It can be seen from Figure 5(a) that a kind of “bubble-like” or “island-like” char is formed when AIHPi is added alone. And there are many holes or gaps in the chars and the scale is relatively large, 5–20  $\mu\text{m}$  approximately. The char morphology is quite different when nanosilica is added alone as shown in Figure 5(b). Most of the char layer appears dense and uniform but unfortunately it is fragile, which can not withstand the impact of the rising bubbles during combustion and will expose the

matrix beneath to fire. As a result, the flame-retardant property of EPDM20-0 is very poor. Interestingly, it seems that the char layer of EPDM20-30 has combined the advantages of the former two kinds of char layers, as shown in Figure 5(c,d). On one hand, this char layer has a certain degree of mechanical strength; and on the other hand, the char layer is more uniform and dense. The scale of the holes is less than 5  $\mu\text{m}$ , smaller than that of the sample of EPDM0-30. This kind of char layer could more efficiently play the role of a physical barrier. The reason could be attributed to the melting and the recrystallization of AIHPi, which is benefited for the contact and the enhancement of the interaction between AIHPi and nanosilica. In conclusion, the synergistic flame-retardant effect between AIHPi and nanosilica mostly resulted from the formation of a more perfect char layer during combustion.



**Figure 4** TG–DSC results of AIHPi in air: (a) TG and DTG; (b) DSC. TG–DSC results of AIHPi in nitrogen: (c) TG and DTG; (d) DSC.



**Figure 5** SEM pictures of the char layer for different samples: (a) EPDM0-30. (b) EPDM20-0. (c) EPDM20-30. (d) Local enlargement of figure (c). \*The pure EPDM burned completely and left almost nothing after burning, so it is not discussed in this article.

#### TG-DSC results

The TG-DSC results for different samples are shown in Figure 6(a-c). It can be seen that the extent of heat release is well corresponding to that of the weight loss in the entire temperature region. Heat release and weight loss are both weak, when temperature is lower than 370°C. Meanwhile, the sharp increase of weight loss corresponds to the relatively strong heat release from 370 to 530°C. Compared with the pure EPDM, the weight loss of EPDM20-0 has decreased but not significantly. As for the value of heat release, although the peak of heat release decreases a lot, the heat release intensity from 370 to 530°C is still relatively strong. This result may be due to the weak strength of the char layer, which cannot withstand the impact of the rising bubbles during combustion, exposing the matrix beneath to fire. In the case of EPDM0-30, both the weight loss and heat release value decrease a lot below 420°C, but a sharp weight loss peak appears above 420°C. Although the peak of heat release decreases a lot, the heat release intensity is still relatively strong from 420 to 500°C. This result may be due to the

ununiformity and large holes of the “bubble-like” or “island-like” char layer, which can not protect the matrix beneath at a higher temperature. The introduction of both AlHPI and nanosilica has solved the problem. It can be seen that the weight-loss rate is weak and the heat release peak value decreases significantly for the sample of EPDM20-30 in the entire temperature region. This result further demonstrates that there is a synergistic flame-retardant effect between nanosilica and AlHPI, and the formation of a dense, strong, and uniform char layer is the key factor for obtaining high flame-retardant materials.

#### CONCLUSIONS

In this study, the flame retardant and mechanical property and the flame-retardant mechanism of EPDM composites blended with AlHPI and nanosilica were investigated.

The results show that the introduction of nanosilica into the EPDM/AlHPI blends can not only further increase flame-retardant property but also improve the value of tensile strength and elongation

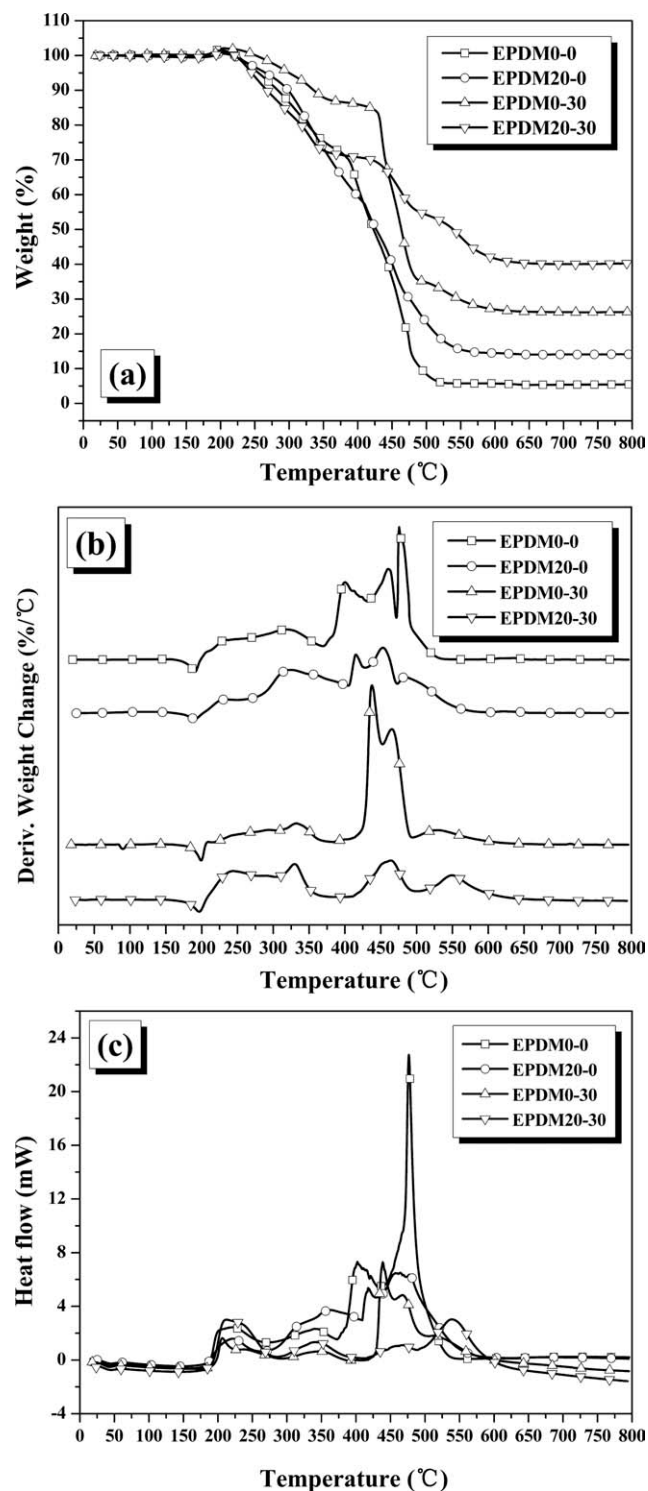


**Figure 6** (a) TG results for different samples. (b) DTG results for different samples. (c) DSC results\* for different samples. \*The value of heat flow was normalized by the mass of each sample.

at break significantly. The results indicate that there is a synergistic effect between AlHPi and nanosilica on the flame-retarded EPDM composite.

The thermal decomposition analysis shows that AlHPi will melt along with oxidation at about

337°C, which is helpful to full contact with nanosilica and to enhance the interaction between them; and will recrystallize above 540°C, which is benefited to enhance the mechanical strength of the char layer. The char morphology analysis by SEM shows that compared with the samples with AlHPi or nanosilica alone, the char layer of the sample with both of them is strong, more uniform and dense, and the holes of the char layer becomes smaller. This may be the key reason for the improvement of the flame-retardant property and the synergistic flame-retardant effect. TG–DSC results show that the sample with both AlHPi and nanosilica has the weakest weight-loss rate and heat-release rate, compared with the samples with either of them. The result further demonstrates that there is a synergistic flame-retardant effect between AlHPi and nanosilica and it can be explained by the formation of a more perfect char layer.

The authors sincerely acknowledge the support of the Knowledge Innovation Program of the Chinese Academy of Science (O84NZ51122).

## REFERENCES

- Wang, Z. Z.; Zhou, S.; Hu, Y. *Polym Adv Technol* 2009, 20, 393.
- Zhou, S.; Wang, Z. Z.; Gui, Z.; Hu, Y. *J Appl Polym Sci* 2008, 110, 3804.
- Morton, M. *Rubber Technology*; R.R. Donnelly & Son Company: Virginia, 1995.
- Lu, H.; Yang, W.; Zhou, S.; Xing, W.; Song, L.; Hu, Y. *Polym Adv Technol* 2010, 21, 113.
- Gallo, E.; Braun, U.; Scharrel, B.; Russo, P.; Acierno, D. *Polym Degrad Stab* 2009, 94, 1245.
- Zhang, Q.; Tian, M.; Wu, Y.; Lin, G.; Zhang, L. *J Appl Polym Sci* 2004, 94, 2341.
- Canaud, C.; Visconteand, L. L. Y.; Reis Nunes, R. C. *Macromol Mater Eng* 2001, 286, 377.
- Ma, Z. L.; Zhao, M.; Hu, H. F.; Ding, H. T.; Zhang, J. *J Appl Polym Sci* 2002, 83, 3128.
- Chiang, W. Y.; Hu, H. C. H. *J Appl Polym Sci* 2001, 82, 2399.
- Braun, U.; Scharrel, B.; Fichera, M. A.; Jager, C. *Polym Degrad Stab* 2007, 92, 1528.
- Braun, U.; Bahr, H.; Sturm, H.; Scharrel, B. *Polym Adv Technol* 2008, 19, 680.
- Kleiner, H. J.; Budzinsky, W.; Kirsch, G. U.S. Pat. 5, 773, 556, 1998.
- Braun, U.; Scharrel, B. *Macromol Mater Eng* 2008, 293, 206.
- Ye, L.; Wu, Q. H.; Qu, B. J. *J Appl Polym Sci* 2010, 115, 3508.
- Takeshi, Y.; Akira, Y.; Gang, W.; Kumi, S.; Kazuhiro, F.; Norio, T. *J Appl Polym Sci A Polym Chem* 2009, 47, 6145.
- Zhu, W. M.; Weil, E. D.; Mukhopadhyay, S. *J Appl Polym Sci* 1996, 62, 2267.
- Zhu, W. M.; Weil, E. D. *J Appl Polym Sci* 1998, 67, 1405.
- Tan, H.; Isayev, A. I. *J Appl Polym Sci* 2008, 109, 767.
- Ichazo, M. N.; Albano, C.; Hernandez, M.; Gonzalez, J.; Carta, A. *Adv Mater Res* 2008, 47–50, 113.

20. Arayaprane, W.; Rempel, G. L. *J Appl Polym Sci* 2008, 109, 932.
21. Sae-oui, P.; Rakdee, C.; Thanmathorn, P. *J Appl Polym Sci* 2002, 83, 2485.
22. Datta, S.; Bhattacharya, A. K.; De, S. K.; Kontos, E. G.; Wefer, J. M. *Polymer* 1996, 37, 2581.
23. Ikeda, Y.; Tanaka, A.; Kohjiya, S. *J Mater Chem* 1997, 7, 1497.
24. Horrocks, A. R.; Anand, S. C.; Sanderson, D. *Polymer* 1996, 37, 3197.
25. Kandola, B. K.; Horrocks, A. R. *Polym Degrad Stab* 1996, 54, 289.
26. Kandola, B. K.; Horrocks, S.; Horrocks, A. R. *Thermochim Acta* 1997, 294, 113.
27. Kandola, B. K.; Horrocks, A. R. *Text Res J* 1999, 69, 374.
28. Kandola, B. K.; Horrocks, A. R. *Fire Mater* 2000, 24, 265.
29. Kandola, B. K.; Horrocks, A. R.; Horrocks, S. *Fire Mater* 2001, 25, 153.